

Mechanical Instability Induced by the Desiccation of Sessile Drops

Y. Gorand,[†] L. Pauchard,[†] G. Calligari,[‡] J. P. Hulin,[†] and C. Allain^{*†}

Laboratoire FAST, Unité Mixte de Recherche Paris VI, Paris XI, and CNRS UMR 7608, Bât. 502, Campus Universitaire d'Orsay, 91405 Orsay Cedex, France, and Grupo de Medios Porosos, F.I.U.B.A., Paseo Colon 850, 1063 Buenos-Aires, Argentina

Received May 6, 2003. In Final Form: February 5, 2004

I. Introduction

The presence of nonvolatile components in a drop gives rise to a complex evolution during its desiccation. In particular, the evolution of the drop shape depends then strongly on the drying conditions and on the composition of the system. For concentrated drops, cracking or warping may take place, leading to patterns that have been the topic of recent studies.^{1–4} Understanding the broad variety of the observed behaviors is highly relevant to coating processes and technologies for applying varnishes or paints. They also represent a particularly spectacular example of surface instabilities in physicochemical systems.

Here we present and discuss the very intriguing shapes of drops of a concentrated polymer solution while they dry. As the solvent evaporates, the outer layer of the drop which has a higher polymer concentration displays a glassy transition; an outer “skin” therefore builds up at the surface. This glassy skin behaves like an elastic solid shell which, however, does not block evaporation; this shell bends as the volume it encloses decreases. Depending on the initial contact angle, a variety of surface distortions has been observed and can be explained by assuming a close relation with the buckling of thin solid sheets.

II. Experimental Section

The experiments were performed using concentrated solutions of dextran (Sigma Aldrich Chemical Co.); the molecular weight is 77,000 g/mol. Solutions were prepared by dissolving a chosen quantity of polymer in water (quality Milli- ρ). For all the experiments reported here, the initial polymer mass fraction, denoted by ω_{p0} , is 0.40 g/g.

The glass transition temperature of our polymer sample, determined by DSC (differential scanning calorimetry), is 220 °C. For a polymer solution, the glass transition temperature is lower than that for the pure polymer and decreases as its concentration decreases.⁵ Thus, for a given temperature, T_{exp} , the glass transition temperature of the solution is smaller than T_{exp} when the polymer concentration, ω_p , is small and larger than T_{exp} when ω_p is large. So, there exists a transition concentration, $\omega_{\text{pg}}(T_{\text{exp}})$, such that the solution is fluid when $\omega_p < \omega_{\text{pg}}(T_{\text{exp}})$ and glassy when $\omega_p > \omega_{\text{pg}}(T_{\text{exp}})$. Thus, during solvent

evaporation, the polymer concentration increases and the solution becomes glassy, although it was initially fluid.

The drops are deposited onto horizontal glass slides using a micropipet. The glass slides are carefully cleaned before use, kept dehydrating in an oven at 120 °C for a chosen time ranging between a few minutes to a few days, and allowed to cool just before use. The duration of dehydration in the oven allows for varying the wetting properties of the glass slides with a great reproducibility: the corresponding contact angle varies over a wide range from $\theta_0 = 10$ to 50°. Still, higher contact angles are obtained using polyethylene slides. The sessile drop geometry represents a well-defined axisymmetric system allowing for reproducible experiments. Variations of the drop shape are observed using a setup allowing accurate recordings of lateral and top views. This setup is placed inside a glovebox inside which the relative humidity, RH, is controlled (RH = 50%).

III. Results and Discussion

Prior to presenting the different shapes which we have observed, let us sum up the main processes involved during the desiccation of a drop of dextran solution.⁴ First, as for colloidal suspensions, the three-phase line at the drop rim is pinned due to a rapid deposition of the polymer on the substrate at the edge;^{6–8} this keeps the drop/substrate contact radius constant in time in contrast with the case of a pure solvent drop which recedes with a constant contact angle. Next, the polymer accumulates near the surface of evaporation, leading to large heterogeneities of concentration. Finally, the rheological properties also change near this surface due to the local increase of the polymer concentration; a rigid, glassy layer builds up at the surface. This skin does not however prevent evaporation, so that the enclosed volume decreases while the contact line remains pinned.

Depending on the initial contact angle of the sessile drop, different time variations of the shape are observed:

For low contact angles ($\theta_0 < \theta_{0c} \cong 30^\circ$), the drop progressively flattens following solvent evaporation (Figure 1a, $\theta_0 = 25^\circ$). The drop shape is not strongly modified and its apex height decreases regularly, as displayed by the spatiotemporal diagram in Figure 2 ($\theta_0 = 25^\circ$).

For all higher contact angles (Figure 1b and c, $\theta_{0c} < \theta_0$), a surface instability takes place and, following θ_0 , this instability results in different drop shapes. Particularly, for intermediate contact angles such as $\theta_{0c} < \theta_0 < \theta_0^* \cong 60^\circ$, the apex height decreases at first and then quickly increases back and reaches a value which may exceed the initial one (Figure 1b, $\theta_0 = 40^\circ$). At the time when the apex height variation begins to differ from the regular trend (Figure 2, $\theta_0 = 40^\circ$), the profiles get distorted (see the profile superposition in Figure 1b). Later, the drop surface area remains constant while its volume keeps decreasing but at a slower rate. At the final stage, the drop has the shape of a “Mexican hat” (see the side view in Figure 1b).⁴ For higher contact angles ($\theta_0^* \cong 60^\circ < \theta_0$), the apex height first decreases following the same trend as in the previous case and then decreases at a faster rate (Figure 2, $\theta_0 = 70^\circ$). In this latter case, the final drop shape (see the side view in Figure 1c, $\theta_0 = 70^\circ$) displays a circular fold, resulting in a dip at the center of the droplet, only observable on profilometry measurements⁹ (Figure 3).

(6) Adachi, E.; Dimitrov, A. S.; Nagayama, K. *Langmuir* **1995**, *11*, 1057.

(7) Parisse, F.; Allain, C. *J. Phys II* **1996**, *6*, 1111.

(8) Deegan, R. D.; Bakajin, O.; Dupont, T. F.; Huber, G.; Nagel, S. R.; Witten, T. *Nature* **1997**, *389*, 827.

(9) Boffa, J. M.; Allain, C.; Hulin, J. P. *Eur. Phys. J.* **1998**, *AP2*, 281.

* Corresponding author. E-mail: allain@fast.u-psud.fr.

[†] Laboratoire FAST.

[‡] Grupo de Medios Porosos, F.I.U.B.A.

(1) Pauchard, L.; Parisse, F.; Allain, C. *Phys. Rev.* **1999**, *E59*, 3737.

(2) Annarelli, C. C.; Fornazero, J.; Bert, J.; Colombani, J. *Eur. Phys. J.* **2001**, *E5*, 599.

(3) Haw, M. D.; Gillie, M.; Poon, W. C. K. *Langmuir* **2002**, *18*, 1626.

(4) Pauchard, L.; Allain, C. *C. R. Acad. Sci., Ser. IV* **2003**, 231–239. Pauchard, L.; Allain, C. *Europhys. Lett.* **2003**, *62*, 897–903.

(5) Plazek, D. J.; Ngai, K. L. The glass temperature. *Physical Properties of Polymers Handbook*; AIP Press: Woodbury, NY, 1996; Part 12.

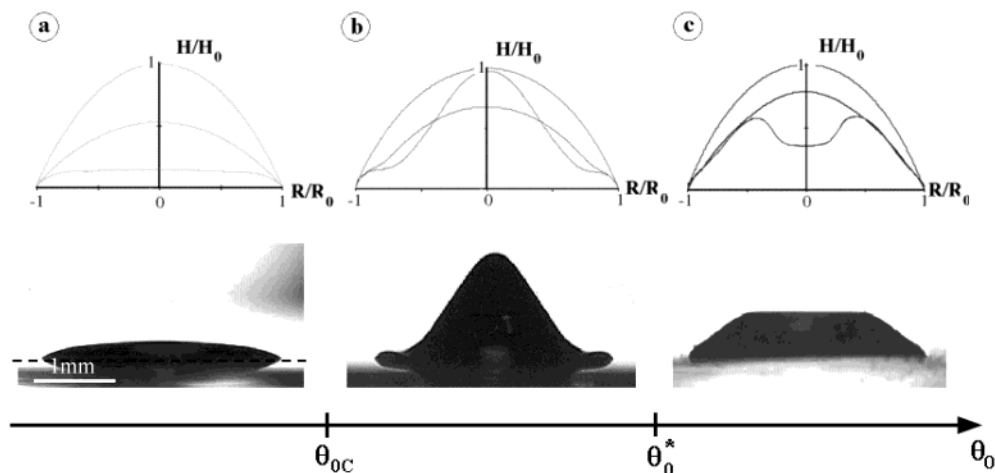


Figure 1. (top) Superposition of dimensionless profiles of sessile drops of dextran solutions recorded at different times during desiccation ($\text{RH} = 50\%$). The time elapsed between two consecutive profiles is 300 s. The initial concentration is the same in all cases ($\omega_{p0} = 0.40$ g/g), while the initial contact angle increases from case a to case c ((a): $\theta_0 = 25^\circ$, $H_0 = 0.70$ mm, $R_0 = 3.16$ mm (stable case). (b): $\theta_0 = 40^\circ$, $H_0 = 1.28$ mm, $R_0 = 3.52$ mm. (c): $\theta_0 = 70^\circ$, $H_0 = 1.85$ mm, $R_0 = 2.64$ mm). Each drop remains axisymmetric. (below) Corresponding digitized side views of the sessile drops taken 1 h after the beginning of the experiment.

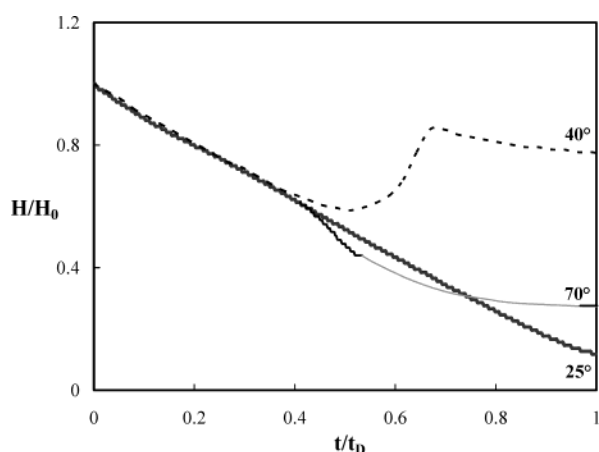


Figure 2. Time variations of the apex height in dimensionless coordinates for the three drop shapes a, b, and c described in Figure 1. H_0 is the drop apex height at $t = 0$, and t_D is the characteristic time of the desiccation process (time needed for the complete desiccation of pure water drops in the same conditions). The values of t_D are 1860, 2400, and 5500 s for $\theta_0 = 25, 40$, and 70° , respectively. In the case of $\theta_0 = 70^\circ$, the dark line corresponds to the experimental measurements, the gray one, to a guide for the eyes, and the horizontal bar at $t/t_D = 1$, to the value H/H_0 that has been measured by mechanical profilometry at $t/t_D \gg 1$.

Surface instabilities observed at large contact angles take place because they allow for the decrease of the enclosed volume despite such constraints as the constant contact base area and the skin rigidity. They can be understood by applying the shell elasticity theory. When the apex height first decreases, compressing the surface as it flattens costs more and more energy and it becomes energetically more favorable to convert a part of the stretching energy into bending energy.¹⁰ Depending on the contact angle, the shape corresponding to the lowest energy is different: there is either a peak or an inversion of curvature leading to the formation of a trough on the axis of the droplet. In this latter case, the trough is limited by a narrow circular ring in which most of the elastic energy is concentrated (Figure 1c). Determining both the radius of curvature, ρ , of the skin, which inverts itself,

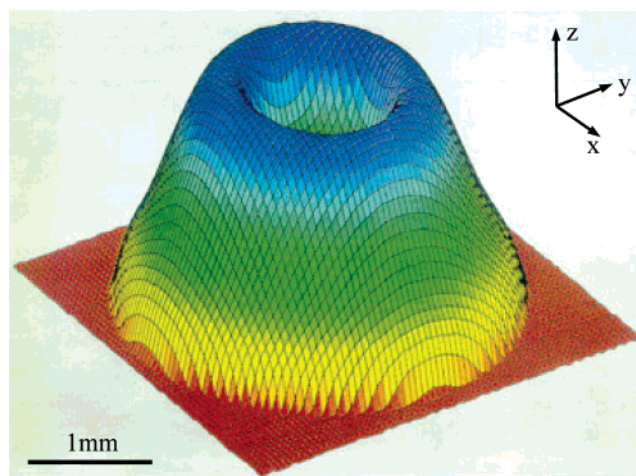


Figure 3. 3D map of the drop corresponding to $\theta_0 = 70^\circ$ (image c of Figure 1). This profile was measured using a mechanical profilometer (length scales are amplified in the z direction to improve legibility).

and the local curvature, $1/\delta$, of the surface allows for an evaluation of the layer thickness, h . Considering a bending deformation extending over a distance of δ and minimizing the bending energy with respect to δ leads indeed to the following relation: $h \cong \delta^2/\rho$ (the prefactor being of the order of 2).¹¹ Using values measured for the circular ring ($\delta \cong 0.40 \pm 0.04$ mm and $\rho \cong 0.80 \pm 0.04$ mm), the thickness is found to be of the order of 0.2 mm in rough agreement with direct measurements (0.4 mm). This latter value was obtained by breaking the drop crust 48 h after the beginning of the experiment and measuring the skin thickness from optical observations. That corresponds to an upper limit of the skin thickness.

The existence of stable or unstable behaviors can be explained from the different evolutions of the drop under desiccation. For stable cases (low contact angles: $\theta_0 < \theta_{0c} \cong 30^\circ$), the desiccation is very fast and in particular too fast for the core of the drop to be still fluid when a glassy skin forms at the drop surface. In other words, the characteristic desiccation time, t_D (t_D is the time needed for water drops to dry completely in the same conditions), is smaller than the time, t_{crust} , that is needed to form a

(10) Timoshenko, S.; Gere, J. M. *Theory of Elastic Stability*, 2nd ed.; McGraw-Hill: New York, 1961.

(11) Pauchard, L.; Rica, S. *Philos. Mag.* **1998**, *B78*, 225.

glassy skin at the drop surface. The drop flattens progressively due to solvent evaporation (Figure 1a): the drop shape is not strongly modified and its apex height decreases regularly, as displayed in Figure 2 ($\theta_0 = 25^\circ$). In another way, if the condition $t_{\text{crust}} < t_{\text{D}}$ is satisfied, that is, for a large contact angle ($\theta_0 > \theta_{0c} \cong 30^\circ$), there is enough time for a glassy skin to build up at the drop surface before complete desiccation and instability takes place during drying. Comparing these two characteristic times suggests a criterion for the occurrence of the instability.⁴

Practically, such a criterion may depend on several parameters. No influence of the drop volume is expected, since the two characteristic times, t_{crust} and t_{D} , are both proportional to water transfer in air and thus to R_0^2 .⁴ On the contrary, the initial polymer volume fraction, ω_{p0} , influences the instability threshold. Indeed, for a given contact angle, when ω_{p0} decreases, the time, t_{crust} , needed to form a glassy skin at the drop surface increases, while the desiccation time remains the same. Since t_{D} increases with θ_0 , the instability threshold corresponds then to a larger value of θ_0 . Last, if the adhesion between the drop and the substrate is reduced, the edge of the drop is not

strongly attached to the substrate any more and the radius of the contact base decreases with time. This modifies the mechanical stresses but does not completely prevent the occurrence of the instability.

IV. Conclusion

Two different modes of buckling instabilities are observed during the desiccation of drops of a polymer solution; depending on the initial contact angle, a peak or a dip builds up at the center. In the present conditions, only axisymmetric distortions were observed; secondary instabilities may also develop for other concentrations or drying rates. Despite their different structures and physicochemical properties, the same type of shape instabilities has been observed in colloidal silica suspensions.¹ Such investigations of mechanical buckling instabilities in physicochemical systems may help to solve a variety of problems related to coating processes or biointerface mechanics.

LA0301947